Journal of
Ceramic Science
and Technology

J. Ceram. Sci. Tech., 07 [01] 29-38 (2016)
DOI: 10.4416/JCST2015-00026
available online at: http://www.ceramic-science.com

Optimization of Nanoparticulate Indium Tin Oxide Slurries for the Manufacture of Ultra-Thin Indium Tin Oxide Coatings with the Slot-Die Coating Process

M. Wegener*, K. Riess, A. Roosen

University of Erlangen-Nuremberg, Department of Materials Science, Glass and Ceramics, Martensstr. 5, D-91058 Erlangen, Germany

received June 15, 2015; received in revised form July 21, 2015; accepted July 31, 2015

Abstract

This paper deals with the optimization of colloidal processing to achieve suitable nanoparticulate indium tin oxide (ITO) slurries for the production of sub-µm-thin ITO coatings with the slot die coating process. For application in printed electronics these ITO coatings, which are composite films consisting of nanoparticulate ITO and a polymeric binder, should offer high flexibility, transparency and electrical conductivity. To preserve their flexibility, the composite films are not subject to any heat treatment, instead they are used as deposited and dried. To achieve very good transparency and electrical conductivity at the same time, the slurries must exhibit excellent dispersivity to result in a dense particle packing during film formation and drying. To reduce materials costs, films with thicknesses of several 100 nm are of interest. Therefore, the slot-die technique was applied as a fast, pre-dosing technique to produce sub-µm-thin ITO/binder composite films. The resulting ITO/binder films were characterized with regard to their key properties such as total transmission and specific electrical resistance. With the colloidal optimization of ethanol- and water-based nanoparticulate ITO slurries using PVP and PVB as binders, it was possible to achieve films of 250 nm in thickness exhibiting high total transmission of ~ 93 % and a low specific electrical resistance of ~ 10 Ω·cm.

Keywords: Nanoparticulate indium tin oxide (ITO), slot-die coating technology, nanocomposite polyvinyl butyral (PVB), polyvinyl pyrrolidone (PVP)

I. Introduction

Transparent, conductive oxide (TCO) materials like indium tin oxide (ITO) or zinc oxide (ZnO) combine the properties of transparency in the visible regime of light and electrical conductivity; they find wide application as transparent electrodes in displays or solar cells [1–5]. Conventionally, ITO films are produced in expensive vacuum-based sputtering processes [6, 7], resulting in the disadvantage of brittle layers; for structuring of the ITO films either a mask is required or structuring is done by means of post-treatment, e.g. by means of laser ablation or different lithography techniques [8–10]. In recent years, lots of research has been done in the field of printed electronics to produce flexible TCO films and structures via less expensive coating and printing approaches [11–13]. In contrast to the TCO films produced in sputter processes, the films and structures produced via a printing process are based on colloidal suspensions of nanoparticles or on precursor solutions. Precursor-based films and structures generally require a post-treatment process to transform the precursor into the desired material; the precursor conversion requires often elevated temperatures and an adapted atmosphere [14, 15]. In the colloidal production approach, the material already exists in its desired confirmation; here the main task is the deagglomeration and stabilization of the particles in suitable solvents and the adjustment of their rheology [16] as well as of their wetting and drying behavior for the subsequent printing process.

Nanoparticulate systems have attracted lots of interest because the properties of the individual particles are in many cases different to their bulk material properties [17] and their size enables the generation of particle-based thin layers and fine structures. In the past, TCO films based on colloidal nanoparticulate TCO suspensions or TCO precursors were produced in spin-coating processes [18, 19]. Straue *et al.* presented the continuous manufacture of TCO films onto a flexible PET film with layer thicknesses in the µm range via the tape casting process [20]. For the continuous manufacture of flexible TCO films in the sub-µm range, the profile rod technique was successfully tested [21]. Both techniques are self-dosing, i.e. slurry properties like viscosity and machine parameters like casting speed, gap of the doctor blade, etc. determine the liquid film thickness applied to a substrate.

This paper describes the production of nanoparticulate TCO films with the slot die coating technique. The slot die coating technique is an established industrial coating process which stands out owing to its high uniform flow distribution over the width of the die and the high homogeneity in the resulting coating [22]; owing to the high coat-

* Corresponding author: moritz.wegener@ww.uni-erlangen.de

ing speeds of up to several hundred meters per min, the slot-die coating technique can be used in roll-to-roll processing, realizing high throughput [23–25]. In contrast to the self-dosing techniques, the slot-die coating is a pre-dosing process, i.e. the amount of liquid which is transferred to a substrate is only dependent on the machine parameters like volume flow, coating speed and geometrical dimensions of the slot die and not on the slurry properties. The liquids have to fulfill certain requirements in dependence on the desired liquid film thickness of the coating, e.g. for the production of liquid films with thicknesses of only a few µm low-viscous slurries exhibiting Newtonian flow behavior are needed. In the past, there has been many scientific publications concerning slot-die coating of polymer solutions [24, 25, 26], but only a few have dealt with the processing of particle-loaded dispersions [27, 28]. In the present study, the slot-die technique is applied to generate nanoparticulate ITO layers in the sub-µm range. With optimization of the colloidal ITO dispersion and slurries and their adaption to the slot-die process, ITO layers were manufactured with improved optical and electrical properties. Because the set-up of the slot-die coating machine requires the preparation of at least 100 ml dispersion or slurry, but the profile rod technique requires only a few milliliters dispersion or slurry, the latter technique was used in pre-experiments to evaluate the influence of the slurry composition on the resulting ITO green films with regard to their optical and electrical properties.

II. Experimental Procedure

(1) Preparation of dispersions and slurries

The ITO dispersions and slurries were based on nanoparticulate ITO powder (Evonik Industries AG, Essen, Germany, density ϱ: 6.51 g·cm^{-3}) with a primary particle size of 19 nm (determined by means of BET measurements, ASAP 2000, Micromeritics Instrument Corp., Norcross, GA, USA). Bi-distilled water, and ethanol p.A. (VWR International GmbH, Darmstadt, Germany, ϱ: 0.79 g·cm^{-3}) were used as solvents. A carboxylic acid (Sigma Aldrich Co., Milwaukee, WI, USA) was applied as dispersing agent. The particle content was set to 20 wt% for all experiments. The dispersions were prepared by treating the mixture of powder, solvent and dispersing agent together with yttrium-stabilized ZrO_2 milling beads (YTZ Grinding Media, Nikkato Corp., Japan) measuring 1 mm, 3 mm and 5 mm in diameter for 24 h in a tumbling mixer (Turbula, Willy A. Bachofen AG, Basel, Switzerland).

Slurries were prepared by adding binder to the deagglomerated dispersions. Polyvinyl pyrrolidone (PVP) K10 and K30 (both Sigma Aldrich Co., Milwaukee, WI, USA, ϱ: 1.11 g·cm^{-3}) and polyvinyl butyral (PVB) B98 (Butvar, Solutia Inc., St Louis, MO, USA) were used as binders. They mainly differ in their molecular weight, which is 40 000 – 70 000 mol/g for PVB B98, 1 000 mol/g for K10 and 44 000 – 54 000 mol/g for K30. The chemical structure of PVB and PVP is shown in Fig. 1. All dispersions and slurries contained 20 wt% ITO, the amount of binder was adapted in relation to the ITO powder. The binder : ITO weight ratios were set to 1 : 8, 1 : 4 and 1 : 2, respectively. The surface tension of the water-based ITO inks was adjusted by the addition of an anionic surfactant (Werner & Mertz GmbH, Mainz, Germany).

(2) Characterization of dispersions and slurries

The dispersions were characterized concerning their mean agglomerate size $x_{50,3}$ by means of dynamic light scattering (DLS) measurements (Nanophox, Sympatec GmbH, Clausthal-Zellerfeld, Germany). The index "3" means that the mean agglomerate size of the volume distribution was determined. In dependence on the milling time and the size of the milling beads used, different mean agglomerate size $x_{50,3}$ values can be achieved [29]. A preparation route leading to a mean agglomerate size $x_{50,3}$ between 150 nm and 180 nm was chosen for all dispersions and slurries that were processed via slot-die coating. Such an agglomerate size ensures the production of highly transparent and conductive ITO/binder films; the use of agglomerates with a smaller size causes an increase of the specific electrical resistance [33].

The rheological behavior of the dispersions and slurries was tested in a rotational rheometer (Physica UDS 200, Paar Physica, Stuttgart, Germany). The viscosity was measured in dependence on the shear rate in a range between 10 and 1000 s^{-1}. The wetting behavior of slurries and dispersions on the PET film (Mitsubishi Polyester Film GmbH, Wiesbaden, Germany) was tested by measuring the surface tension according to the Pendant-Drop-Method (Sessile-Drop-Method, Contact Angle System OCA 30, Dataphysics Instruments GmbH, Filderstadt, Germany).

(3) The profile rod technique (PRT)

The working principle of the profile rod technique is shown in Fig. 2; the dispersion or slurry is placed in front of a rod bar. The rod bar is placed in a fixed position above the moving substrate film and the slurry is forced by the moving carrier film to pass through the gaps. After passing the rod bar, a smooth and homogeneous film should develop. Low-viscous dispersions or slurries showing little shear thinning or even pure Newtonian flow behavior can be processed. For the production of the ITO coatings, a rod bar with a gap height of 4 µm was used and a coating speed of 6 m/min was applied. All samples were dried in ambient conditions.

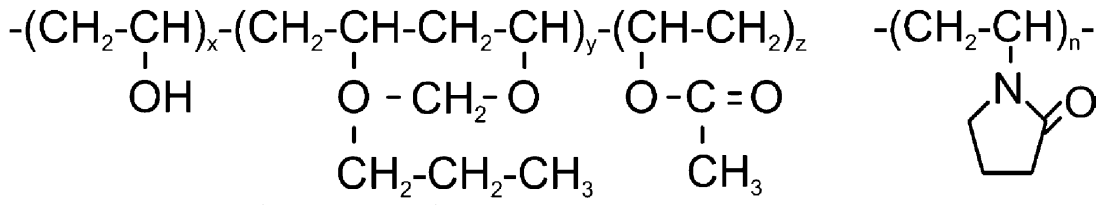

Fig. 1: Chemical structure of PVB (left) [1] and PVP (right) [1].

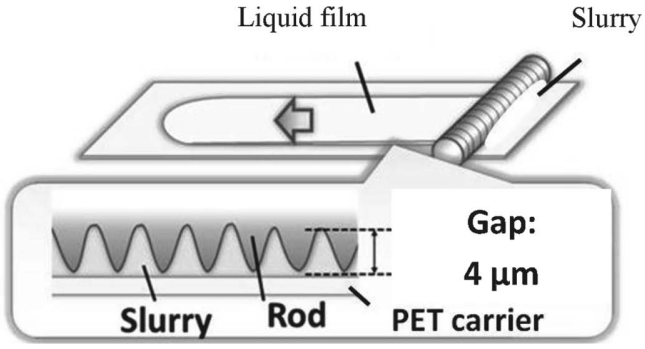

Fig. 2: Schematic showing the working principle of the profile rod technique, adapted from [1].

(4) The slot-die coating technique

The working principle of the slot-die coating technique is shown in Fig. 3. A pump transports the dispersion or slurry through a pipeline system into the slot-die. A substrate that runs beyond the slot-die is continuously coated. The liquid film thickness h transferred to the substrate is defined by the flow rate $\dot{m}$ of the liquid, the substrate velocity v, the width of the slot-die b and the density of the slurry or dispersion ϱ, cf. Equation 1.

$$h = \frac{\dot{m}}{vb\rho} \quad (1)$$

A slot-die (FMP Technology GmbH, Erlangen, Germany) with a width of 100 mm and a slot gap of 400 µm, a syringe pump and a substrate transport system (self-made) was used for the production of ITO coatings. The flow rate was controlled with a software-controlled syringe pump. The "bead-mode" was chosen as coating mode [30]; here, the distance between substrate and slot-die is around 80 µm. Films with wet film thicknesses between 2.5 µm and 100 µm were produced; in general, thicknesses down to 5 nm can be produced if particle-free precursor-solutions are used. Coating speeds of 0.5 m/min and 2 m/min were realized; higher coating speeds were not possible owing to restrictions of the transport system used. All samples were dried in ambient conditions.

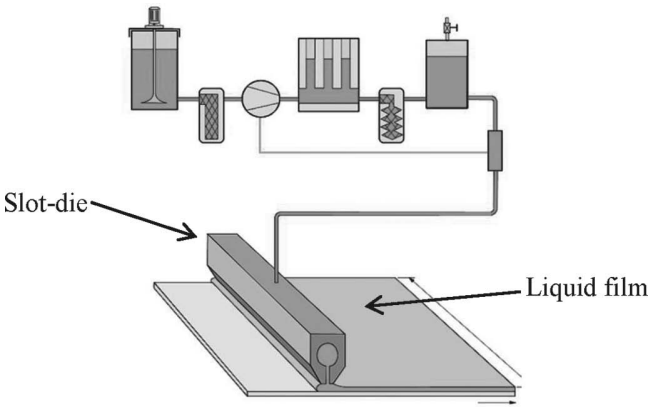

Fig. 3: Schematic working principle of the slot-die technique adapted from [25].

(5) Characterization of coatings

The four-point measurement principle (current source: Type J4, Knick Elektronische Messgeräte GmbH & Co. KG, Berlin, Germany; multimeter: Type 34401 A, Hewlett-Packard Co., Palo Alto, CA, USA) was used to measure the electrical resistance values of the ITO coatings. The optical properties were determined in an UV/Vis spectrometer (Lambda 950, Perkin Elmer, Inc., Waltham, MA, USA). Total transmission measurements in a range between 250 nm and 2500 nm were recorded with a measurement interval size of 3 nm. The thickness of the ITO coating was measured with confocal microscope measurements (microsurf custom microscope, NanoFocus AG, Oberhausen, Germany). The microstructure analysis was performed by means of scanning electron microscopy (Helios NanoLab 600i and Quanta 200, both: FEI, Hillsboro, Oregon, USA).

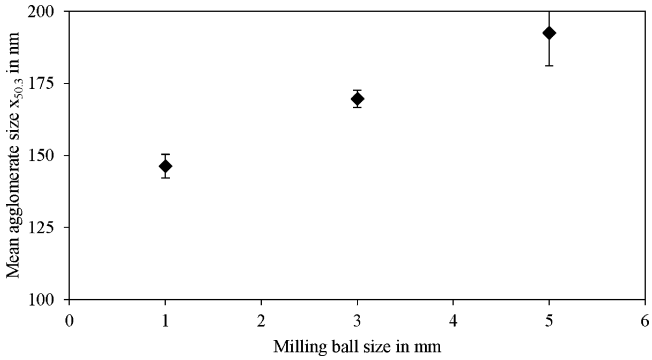

Fig. 4: Mean agglomerate size $x_{50,3}$ of an ethanol-based ITO dispersion, containing 6 vol% ITO, as function of the milling bead size. Dispersing period: 24 h.

III. Results and Discussion

(1) Colloidal processing

The electrical and optical properties of ITO green films are a function of the mean agglomerate size $x_{50,3}$ of the corresponding dispersions and slurries [33]. In ceramic processing, the material properties are often improved when agglomerates are completely deagglomerated. However, nanoparticulate ITO green films offer the highest transmission values and lowest resistivity values when their ITO agglomerates, forming the nanoparticulate network, exhibit mean agglomerate size values $x_{50,3}$ between 150 nm and 180 nm; a further reduction of agglomerate size is counterproductive. The reason for this behavior will be discussed in the following sections. Understanding and control of the colloidal processing of the nanoparticulate ITO systems was therefore essential to achieve ITO green films with optimized electrical and optical properties. The influence of the milling bead size on the mean agglomerate size $x_{50,3}$ after a dispersing period of 24 h is shown in Fig. 4. The achieved mean agglomerate size $x_{50,3}$ decreased with decreasing milling bead size, e.g. the usage of milling ball with a diameter of 5 mm led to a mean agglomerate size $x_{50,3}$ of around 190 nm whereas a milling bead size of 1 mm caused a mean agglomerate size of around 140 nm. A smaller milling bead size corresponds to a higher milling frequency, assuming that the milling bead mass stays constant, and to an improved deagglomeration process.

The mean agglomerate size $x_{50,3}$ not only depends on the size of the milling beads but also on the dispersing period as shown in Fig. 5 for an ethanol-based ITO dispersion processed with 1-mm-diameter milling beads. A dispersing period of 24 h led to a mean agglomerate size $x_{50,3}$ of around 140 nm; doubling the dispersing period to 48 h caused a decrease of the mean agglomerate $x_{50,3}$ size by 30 nm to around 110 nm. Further lengthening of the dispersing period to 72 h had no significant influence on the mean agglomerate size $x_{50,3}$, cf. Fig. 5.

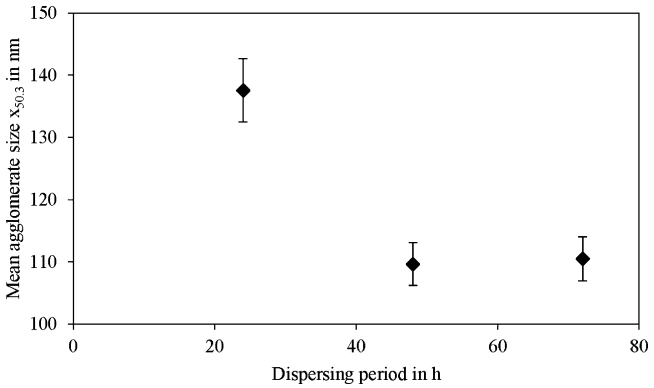

Fig. 5: Mean agglomerate size $x_{50,3}$ of an ethanol-based ITO dispersion, containing 6 vol% ITO, as function of the dispersing period. Milling bead size: 1 mm.

A mean agglomerate size $x_{50,3}$ between 150 nm and 180 nm is most favorable to obtain ITO green films with high optical transparency and improved electrical properties as shown in the literature [33]. Therefore milling beads with 3 mm diameter and a processing period of 24 h were chosen for the preparation of ITO dispersions and slurries presented in the following sections.

(2) Rheological characterization of dispersions and slurries

The production of sub-µm thin layers with the slot-die coating technique requires low-viscous Newtonian fluids. Fig. 6 shows the viscosity at 1000 s^{-1} of ethanol-based 20 wt% ITO slurries in dependence on their binder : ITO ratio. The influence of the amount of the binder PVB B98 (40 000 – 70 000 mol/g) and the amount of the binder PVP with two different molar weights (K10:1 000 mol/g, K30: 44 000 – 54 000 mol/g) is presented. An increasing amount of binder as well as an increase of the molecular weight of the binder, e.g. by changing from PVP K10 to PVP K30, resulted in an increase in the viscosity. Additional measurements showed that at high binder contents (binder to ITO weight ratio 1 : 2), the slurries lost their ideal Newtonian flow behavior and became shear thinning; high molecular weight binder like PVP K30 and PVB B98 caused a stronger shear shinning behavior than the low molecular weight binder PVP K10.

In general, water-based ITO slurries showed the same viscosity behavior in dependence on the type and amount of binder as the ethanol-based slurries; the viscosity values measured at a shear rate of 1000 s^{-1} are shown in Table 1. The binder PVB B98 could not be used in water-based ITO slurries because PVB is not soluble in water. For the chosen slot-die coating application mode, only low-viscous liquids are of interest; the viscosity should not exceed a value of approximately 15 mPa·s.

(3) Adaption of the surface tension of water-based ITO slurries

Fig. 7 shows the surface tension of a water-based 20 wt% ITO dispersion and of slurries with different amounts of surfactant (S). The ITO dispersion had a surface tension of around 70 mN/m which is almost similar to the surface tension of pure water (72 mN/m). The surface tension of a water-based 20 wt% ITO slurry with a PVP K30 : ITO ratio of 4 was around 55 mN/m and showed insufficient wettability on the PET substrate. In comparison, the ethanol-based inks exhibited a surface tension of around 23 mN/m, which is comparable to pure ethanol, and showed good wettability. The addition of the less-polar binder PVP reduced the surface tension of the highly polar water. The surface tension of the slurry could further be adjusted with the addition of 3 wt% surfactant. The surfactant reduced the surface tension of the slurry to around 35 mN/m, see Fig. 7.

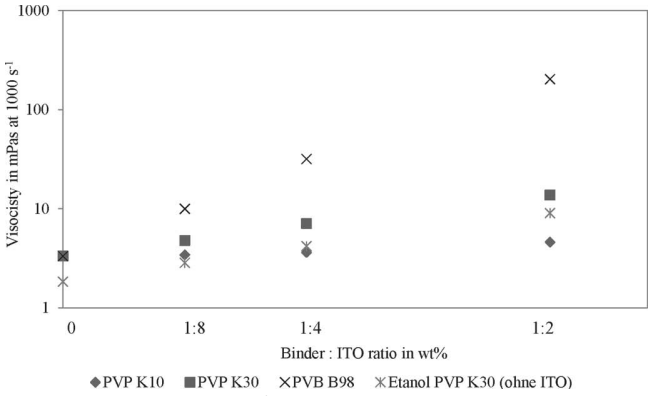

Fig. 6: Viscosity (at 1000 s^{-1}) of ethanol-based 20 wt% ITO slurries in dependence on the binder : ITO ratio for different types of binder.

Table 1: Viscosity in mPas at 1000 s^{-1} for ethanol- and water-based 20 wt% ITO slurries with different type and amount of binder; the slurry compositions marked with a "*" were used for the slot-die coating experiments.

Solvent	Binder:ITO	PVP K10	PVP K30	PVB B98
Ethanol	0*	3.3	3.3	3.3
	1:8	3.4	4.8	10.0
	1:4	**3.6***	**7.1***	31.2
	1:2	4.6	13.8	203.9
Water	0	2.4	2.4	2.4
	1:8	2.9	3.4	-
	1:4	**3.1***	**5.3***	-
	1:2	4.2	11.2	-

A decrease in the surface tension of the liquid σ_{LG} will lead to a decrease of the contact angle α according to Young's equation [31], cf. Equation 2, assuming that the sur-

face tension of the substrate σ_{SG} and the surface tension of the substrate-liquid-interface σ_{SL} are both constant [32].

$$\frac{\sigma_{SG} - \sigma_{SL}}{\sigma_{LG}} = \cos\alpha \qquad (2)$$

The results of pre-tests confirmed that the addition of such small amounts of surface active agent had no negative influence on the optical and the electrical properties of the ITO coatings.

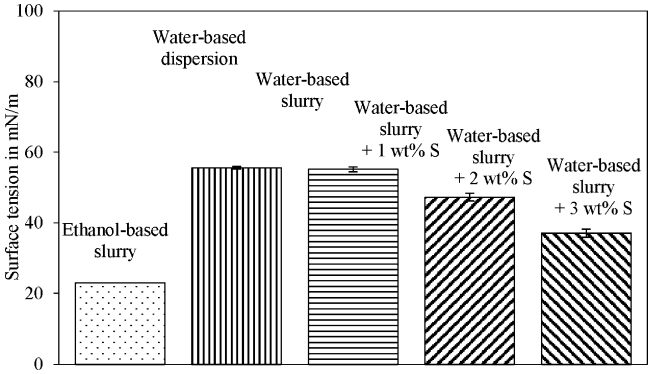

Fig. 7: Surface tension of water-based 20 wt% ITO dispersion and of water-based 20 wt% ITO slurries (PVP K30 : ITO ratio = 1 : 4) with different amounts of surfactant (S).

(4) Characterization of the ITO films produced with the PRT

The set-up of the slot-die coating machine required the allocation and the preparation of at least 100 ml dispersion or slurry; for the production of coatings with the profile rod technique only a few milliliters dispersion or slurry were required. Therefore, the profile rod technique was used to evaluate the influence of the slurry composition on the resulting ITO green films with regard to their optical and electrical properties. 20 wt% ITO slurries based on water and ethanol as solvent were used to produce ITO coatings. It was found that the key properties of the ITO green films, the specific electrical resistance and the transmission, were mainly dependent on the ITO : binder ratio in the green film. The solvents acts only as non-permanent carrier medium and had only a minor influence on the resulting ITO green film properties. Therefore, only the electrical and optical properties of the ITO green films produced from ethanol-based systems are presented; for water-based ITO slurries and ITO films, almost the same values resulted with regard to their specific resistance and inline-transmission. All ITO films obtained by means of the PRT had film thicknesses of around 1.3 µm after drying.

(a) *Electrical characterization*

Fig. 8 shows the specific resistance of ITO green films in dependence on the binder : ITO ratio of the ethanol-based 20 wt% ITO slurries used. An increased binder : ITO ratio in the slurry resulted in an increased binder volume in the green film after drying. The specific electrical resistance of ITO green films produced from pure ITO dispersions was around 30 Ω·cm. An addition of binder up to a binder : ITO ratio of 1 : 4 reduced the specific resistance to around 3 Ω·cm, independent of the type of binder chosen. A further increase of the binder content increased the specific electrical resistance again. This behavior was also found by Königer *et al.* for the addition of PVP K30 to ethanol-based ITO slurries [33]; obviously this effect is also transferable to the binder PVB (see Fig. 5). Königer *et al.* explained the improvement of the electrical conductivity based on induced shrinkage of the ITO percolation network with the addition of binder that led to better inter-agglomerate contacts during drying, improving the electrical conductivity of the ITO film. The addition of larger binder amounts resulted in the formation of thicker insulating layers between the agglomerates.

(b) *Optical characterization*

The inline-transmission values at 600 nm in % of ITO green films in dependence on the binder : ITO ratio of the corresponding ITO slurries are shown in Fig. 6. All films had nearly the same thickness of around 1.3 µm. The films produced from the pure ITO dispersion showed the highest inline transmission of 88 % at 600 nm. Independent of the type of binder, a similar optical inline transmission behavior of the ITO films in dependence on the binder content was observed. A small addition of binder (binder : ITO ratio of 1 : 8) led to a drop in the inline transmission. At higher binder content (binder : ITO ratio of 1 : 4 or 1 : 2) the inline transmission increased to almost the same values as was the case for the ITO film produced from the pure ITO dispersion.

(c) *Microstructure analysis*

The optical behavior of ITO green films strongly depends on their microstructure. The microstructure is influenced by the mean agglomerate size of the agglomerates and their packing behavior [33], i.e. an increasing agglomerate size resulted in a less densely packed nanoparticulate ITO network and reduced the inline transmission of the ITO green films. The optical behavior of the ITO green films presented in Fig. 10 can be traced back to the mode of operation of the binders. A very homogeneous nanoparticulate ITO film developed by means of drying pure and well-dispersed ITO dispersions, see Fig. 10a. The pores of the nanoparticulate network were so small that they did not interact with the visible light, allowing high transmission values.

When binders are added to an ITO dispersion, the binder molecules adsorbed on the surface of the ITO primary agglomerates and form ITO/binder agglomerates during drying, as shown in the literature [34]. The optical behavior of ITO green films changes as a function of the agglomerate size and their packing behavior, as reported in the literature [33], e.g. the inline transmission drops with increasing agglomerate size. Binders like PVP and PVB are known to densify to packed structures during drying as a result of shrinkage [38]. When only small amounts of binder were added (here: 5 wt% binder), the binder acted like glue between the primary agglomerates and led to the formation of comparably coarse ITO/binder agglomerates during drying, causing a more inhomogeneous packing, cf. Fig. 10b. Increasing binder content (here: 10 wt% and

15 wt%) caused an increase of the binder envelope thickness around each primary agglomerate. A thick binder envelope acted as a steric hindrance and increased the average distance between each primary agglomerate during drying; in this case, light experienced a similar scattering as in pure nanoparticulate ITO Systems. The preservation of the agglomerate state of a pure ITO dispersion in ITO/PVP films with high binder contents (here: 10 wt% and 15 wt%) therefore resulted in optical properties comparable to pure ITO films.

The addition of binder not only influenced the agglomerate size but also the drying stresses and led to the formation of cracks. Normally, binders are used to provide strength and flexibility for green tapes [34]. In this study, cracks were observed when the binder PVP K10 and K30 were added to the dispersion. The influence of the amount of PVP K10 on the crack formation is shown in Fig. 11; small cracks were observed when low amounts of PVP K10 (here: binder : ITO ratio = 1 : 8) or medium amounts (here: binder : ITO ratio = 1 : 4) were added. With an increase in the binder content, the size of the cracks rose but the number of cracks was reduced, c.f. Fig. 11c. Obviously, the size and the number of the cracks were dependent on the magnitude of the drying stresses which seems to increase with increasing binder content.

The influence of the molecular weight of the binder on the crack development becomes visible in a comparison of Fig. 11b and Fig. 12a (the same amount of binder was added in both cases); the addition of PVP K30 (Fig. 12a) caused cracks with larger size and lower number than the same amount of PVP K10 (Fig. 11b) did.

The formation of cracks depends on the magnitude of the drying stresses, as already mentioned. However, a comparison of the micrographs of ITO/binder films manufactured with the binders PVP K30 and PVB B98, which exhibit almost the same molecular weight, showed that no cracks were formed when PVB B98 was used. The difference in the film formation was traced back to the different chemical structures of PVP and PVB, cf. Fig. 1. It is assumed that the reactive OH-groups of the PVB molecules allowed stronger interaction between neighboring PVB molecules and ITO particles [35], adsorbing higher drying stresses than PVP molecules did. Fewer interactions between the PVP molecules are expected owing to the absence of reactive OH-groups.

Independent of the choice of binder, a binder : ITO ratio of 1:4 led to the lowest specific resistance values in this experimental series (see Fig. 8). Even though many cracks were observed by means of SEM microscopy for the usage of PVP K10 and K30 the electrical properties of the ITO/PVP and ITO/PVB films were similar. The low specific resistance of the ITO/PVP coatings led to the conclusion that only the surface of the ITO coatings was damaged by cracks. A continuous conductive path for the electron movement must exist in the lower part of the coatings. As a conclusion, a proper choice of the molecular weight and type of binder allowed the prevention of crack development, e.g. usage of PVB instead of PVP.

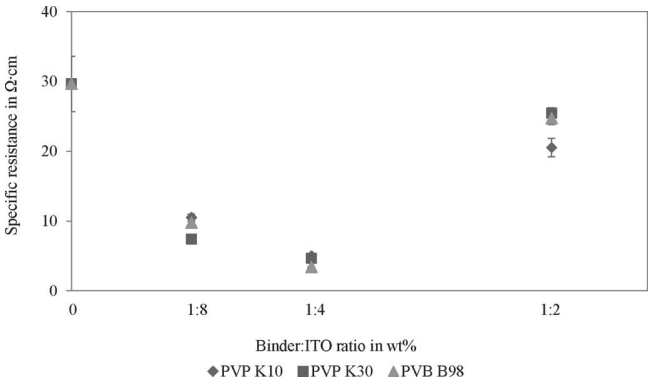

Fig. 8: Specific resistance of ITO green films in dependence on the binder : ITO ratio of ethanol-based 20 wt% ITO slurries that were used for the manufacture of the ITO green films.

(5) Slot-die coating

The rheological characterization of the ITO dispersions and slurries as well as the evaluation of the corresponding ITO and ITO/binder films concerning their optical and electrical properties in the previous sections made it possible to extract a small number of slurries worth using in the slot-die coating process. For the production of dried films in the sub-µm range, liquid films with a thickness of a few µm had to be deposited on a substrate. The manufacture of very thin liquid films with the slot-die coating technique in the bead mode required slurries with low-viscous Newtonian flow behavior, i.e. all slurries that had a binder : ITO ratio of 1 : 2 were not suitable for coating experiments. The optical as well as the electrical characterization of the ITO films (see Fig. 8 and Fig. 9) showed that pure ITO dispersions as well as ITO slurries with a binder : ITO ratio of 1 : 8 exhibited worse properties than ITO films manufactured from a slurry with a binder : ITO ratio of 1 : 4; i.e. only ITO slurries with a binder : ITO ratio of 1 : 4 were processed with the slot-die coating technique; these slurries are marked with a "*" in Table 1.

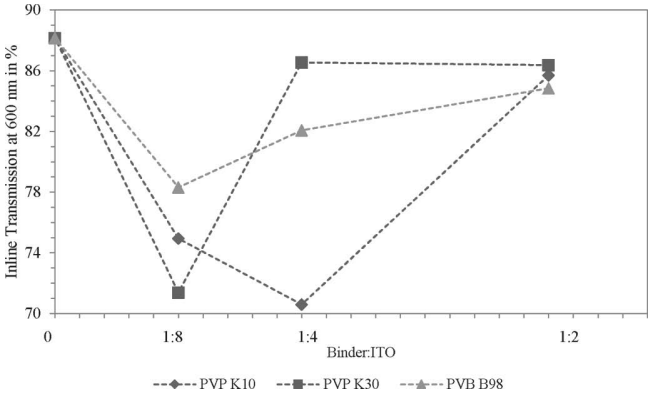

Fig. 9: Total transmission at 600 nm in % of ITO green films in dependence on the binder: ITO ratio of ethanol-based 20 wt% ITO slurries.

The slot-die coating technique, which allows easy and exact control of the liquid film thickness with the adjustment of the volume flow rate and the coating speed was used to produce ITO and ITO/binder films with different film thicknesses. The electrical and optical properties of the dried ITO films and ITO/binder films as a function

of the dried film thickness were similar, independent of the choice of the solvent (water, ethanol) and the type of binder (PVP, PVB) during processing. For these reasons, in the following three sections only the electrical and optical properties of ITO/PVP K30 films processed by slot-die coating experiments from an ethanol-based 20 wt% ITO slurry with an binder : ITO weight ratio of 1 : 4, are presented. The influence of the solvents, water or ethanol, on the crack-formation of ITO/PVP K30 green films is discussed in section III(4)(d).

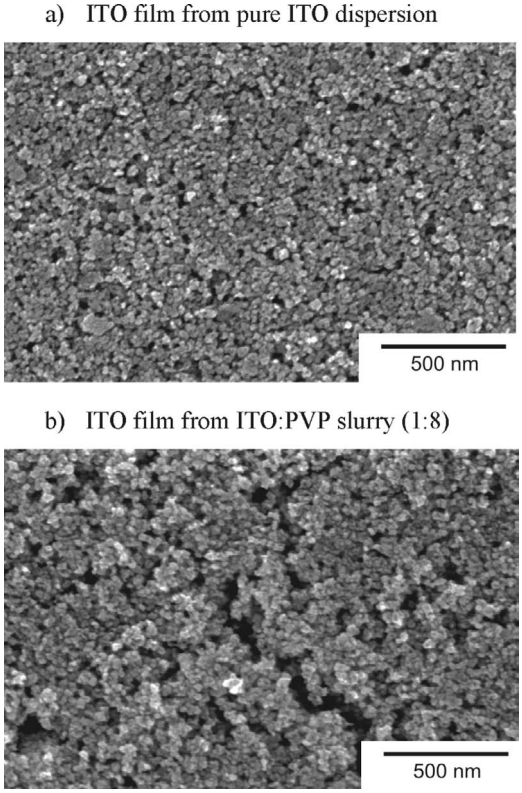

Fig. 10: SEM micrograph of the surface of dried ITO and ITO/PVB green films.

(a) ***Production of sub-µm thin coatings***

The layer thickness of dried ITO films produced from an ethanol-based 20 wt% ITO slurry with a PVP K30 : ITO ratio of 1 : 4 in dependence on the applied liquid film thickness is shown in Fig. 13. A coating speed of 0.5 m/min and 2 m/min was used for the experiments. The applied liquid film thickness was varied between 2.5 µm and 100 µm and resulted in layer thicknesses of dried ITO films between 250 nm and 6 µm, i.e. an average drying shrinkage of around 92 % was observed. A linear dependence between the applied liquid film thickness and the layer thickness of dried ITO films could clearly be seen.

(b) ***Electrical properties in dependence on the film thickness***

The specific electrical resistance of dried ITO films produced from an ethanol-based 20 wt% ITO slurry with a PVP K30 : ITO weight ratio of 1 : 4 in dependence on the dried layer thickness is shown in Fig. 14. ITO films with a layer thickness between 1 µm and 6 µm showed nearly similar specific resistance values of around 2 Ω·cm to 4 Ω ·cm. In this thickness range the specific electrical resistance seems to be independent of the film thickness, which led to the conclusion that the quality and the microstructure of the ITO films were similar in this layer thickness window. ITO films with a film thickness of around 500 nm exhibited a specific electrical resistance of around 6 Ω·cm. A further reduction of the film thickness to around 250 nm led to an increase of the specific electrical resistance value to around 12 Ω·cm. The rising specific electrical resistance with decreasing layer thickness was caused by a decline of the microstructure quality compared to ITO films with a higher film thickness. The ITO slurries used for the coating experiments contained ITO agglomerates with a mean agglomerate size of around 150 nm – 180 nm, i.e. an ITO film with a layer thickness of around 250 nm is built up by only a few agglomerates; already small packing failures will lead to a reduction of the number of electron pathways in the percolation network. The processing of slurries with smaller agglomerates would allow the production of films with even lower thickness and suitable packing density. However, the electrical properties of nanoparticulate ITO green films are a function of the agglomerate size as shown in the literature [33]; the electrical properties of ITO green films become worse with the processing of slurries with smaller agglomerate size. A reduction of the agglomerate size leads to a rise in the number of inter-agglomerate grain boundaries; each inter-agglomerate grain boundary acts as a hindrance to the electron movement and causes an increase of the electrical resistance. The agglomerate size determines the electrical properties of ITO green films and limits therefore also the minimum film thickness. ITO/binder films with low specific resistance values between 2 and 4 Ω·cm were processed down to film thicknesses of around 750 nm; at even lower film thicknesses the specific electrical resistance increased again.

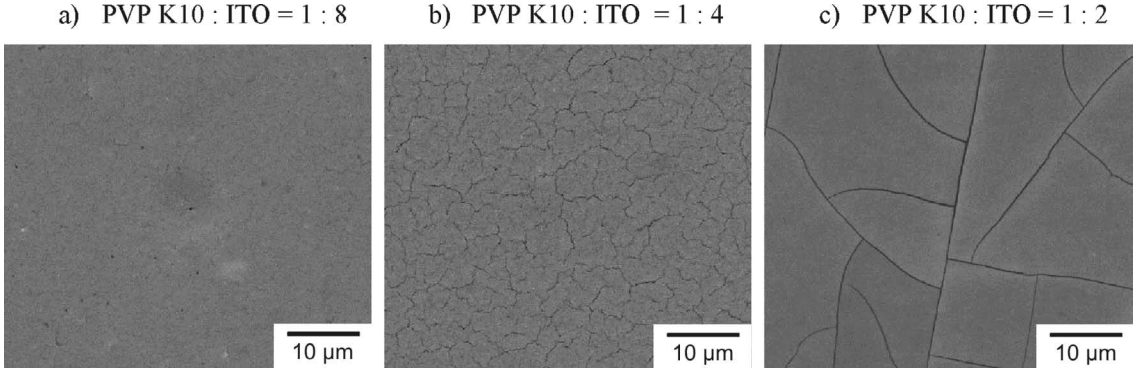

Fig. 11: SEM micrographs of ITO/PVP K10 coatings with different PVP K10 : ITO ratios.

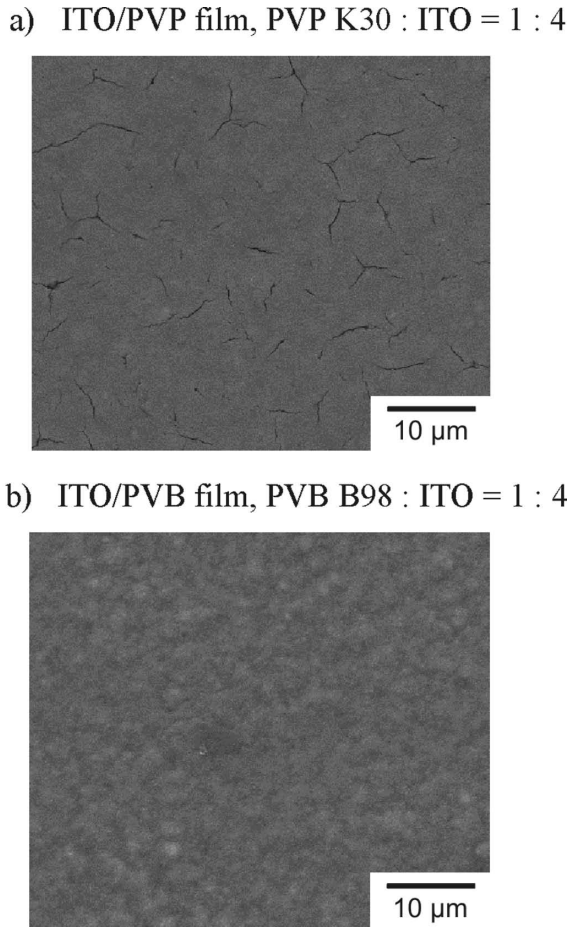

Fig. 12: SEM micrographs of ITO/PVP (a) and ITO/PVB coating (b); the ITO: binder ratio is 1 : 4 in both cases.

(c) ***Optical properties in dependence on the film thickness***

The total transmission of dried ITO films at a wavelength of 600 nm, produced from an ethanol-based 20 wt% ITO slurry, in dependence on the dried layer thickness is shown in Fig. 15. The total transmission of ITO layers with a layer thickness of around 250 nm laid at around 93 % and decreased down to 82 % for ITO films with a film thickness of around 6 µm. In a layer thickness range between 250 nm and 6 µm the total transmission of ITO layers at a wavelength of 600 nm decreased almost linearly; a higher ITO layer thickness resulted in a higher number of ITO agglomerates which interacted with the transmitting light, causing higher absorption.

(d) ***Comparison of the microstructure of ITO/PVP K30 films processed with water- and ethanol-based slurries***

PVP has the advantage that it can be used in ethanol- and water-based dispersions. Fig. 16 shows SEM micrographs of ITO/PVP K30 green films produced from a) ethanol-based and b) water-based slurries processed with a liquid film thickness of 5 µm, 10 µm and 20 µm, respectively. The development of cracks in dependence on the film thickness was comparable for ITO/PVP K30 films manufactured from ethanol- and water-based slurries. No cracks were visible in thin ITO/PVP K30 films (film thickness: ~ 500 nm). ITO/PVP K30 films with a thickness of between 780 nm and 860 nm exhibited crack formation. An increase of the film thickness to around 1800 nm to 1900 nm pronounced the development of larger cracks. Concerning crack size, the ITO/PVP K30 films processed from ethanol-based slurries exhibited much smaller cracks than ITO/PVP K30 films processed from water-based slurries. The stronger crack formation in films produced from water-based slurries can be traced back to the higher drying stresses which are caused by the high surface tension of water. The surface tension of water used for the water-based slurries was reduced by surfactants; nevertheless the surface tension had still values close to 35 mN/m which was nearly twice that high as for ethanol (21 mN/m).

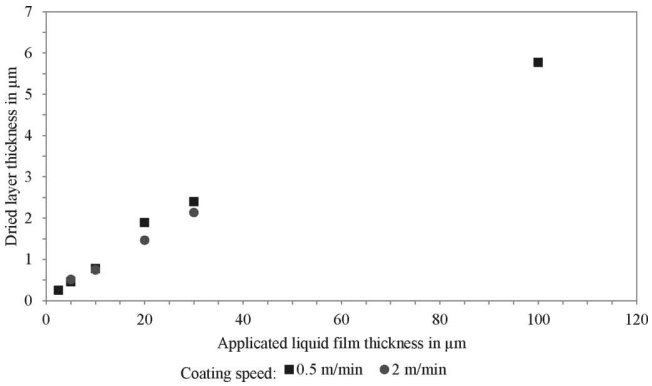

Fig. 13: Layer thickness of dried ITO films in dependence on the applied liquid film thickness manufactured from an ethanol-based 20 wt% ITO slurry, PVP K30 : ITO ratio of 1 : 4.

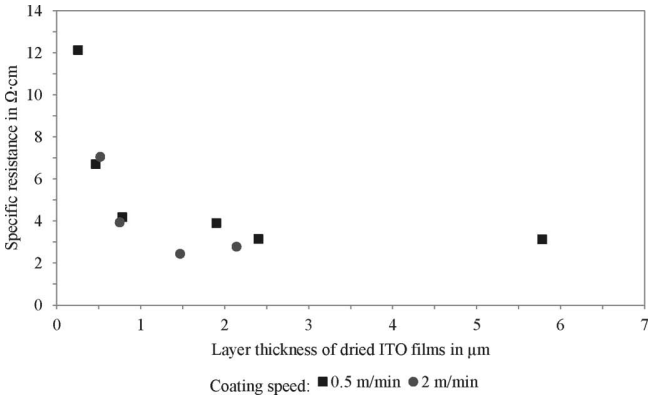

Fig. 14: Specific resistance of dried ITO films in dependence on the dried film thickness produced from an ethanol-based 20 wt% ITO slurry, PVP K30 : ITO ratio of 1 : 4.

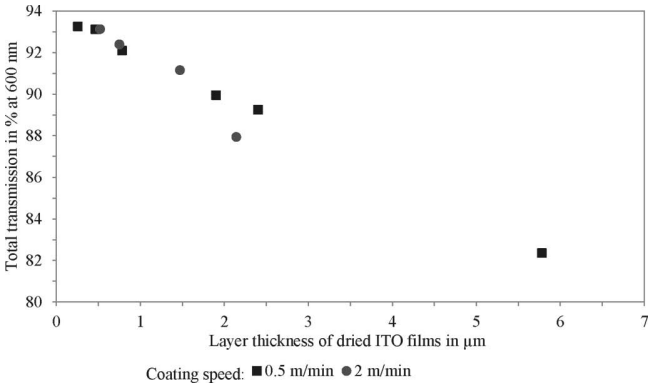

Fig. 15: Total transmission of dried ITO films in dependence on the dried film thickness manufactured from an ethanol-based 20 wt% ITO slurry, PVP K30 to ITO ratio of 1 : 4.

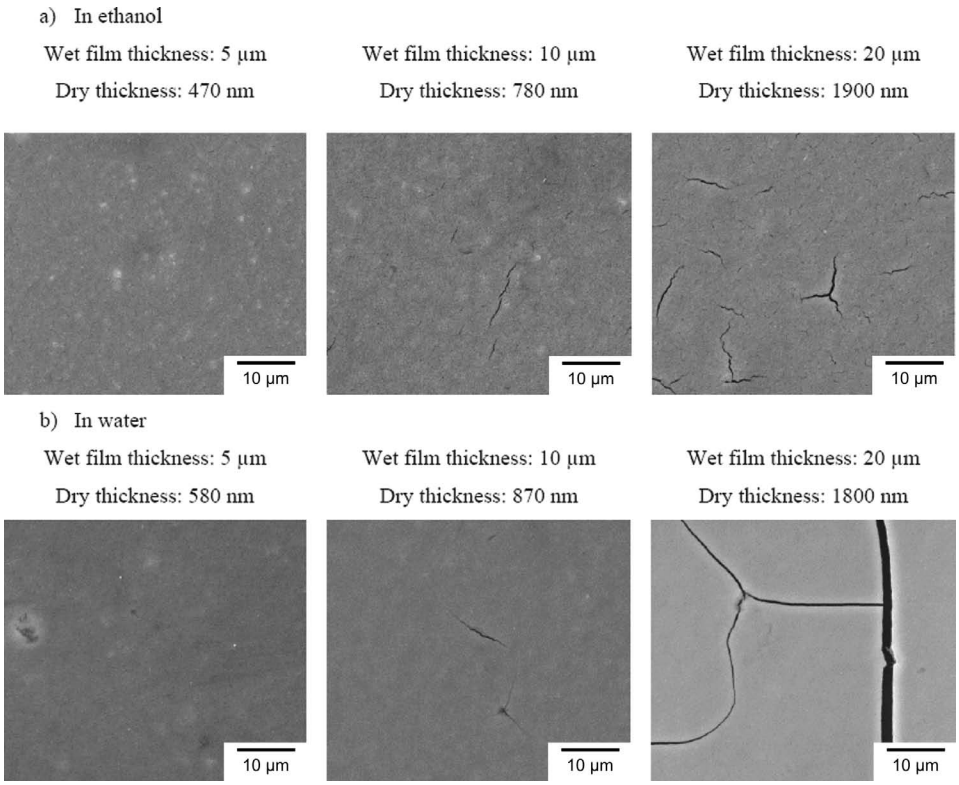

Fig. 16: SEM micrographs of ITO/PVP K30 films manufactured with a liquid film thickness of: 5 µm, 10 µm and 20 µm from an ethanol-based (a) and a water-based slurry (b).

IV. Conclusions

This paper deals with the optimization of nanoparticulate ITO slurries for the production of ITO films by means of the slot-die coating process. The profile rod technique was used for preliminary coating tests to evaluate the influence of the slurry composition on the ITO film properties. It was found that a binder : ITO weight ratio of 1 : 4 led to ITO/binder composite films with the best properties concerning transmission and specific electrical resistance. Microstructure analysis revealed crack formation in the ITO/binder nanocomposite films but could be avoided with proper selection of the solvent and the type and amount of binder, maintaining high optical transparency and good electrical conductivity of the films. Both coating techniques required low-viscous Newtonian liquids, i.e. slurries which could successfully be processed in the profile rode technique could also be used in the slot-die coating processes. The rheological behavior was optimized based on the proper choice of the ITO powder content, the type and amount of binder and the solvent. Water- and ethanol-based ITO slurries that allowed the production of sub-µm-thin nanoparticulate ITO films with the slot-die coating technique by applying a coating speed of 2 m/min were developed. The coating speed was limited by the machine used; in general, coating speeds up to several hundred meters/min can be realized with the slot-die coating technique [25–27]. The wet films exhibited a drying shrinkage of 90 %, resulting in film thicknesses between only 250 nm and 6 µm. These films showed specific resistance values down to 2 – 3 Ω·cm and inline transmission values of around 90 % at a wavelength of 600 nm.

Acknowledgment

The financial support of the German Research Foundation (DFG, Graduiertenkolleg 1161) as well as the support of the ITO powder from our industrial partner Evonik Industries AG, Essen, Germany, are gratefully acknowledged.

References

1 Minami, T.: Transparent conducting oxide semiconductors for transparent electrodes. Semicond. Sci. Tech., 20, 35 – 44, (2005).

2 Granqvist, C.G., Hultaker. A.: Transparent and conducting ITO films: new developments and applications, Thin Solid Films, 411, 1 – 5, (2002).

3 Liu, H., Avrutin, V., Izyumskaya, N., Özgur, Ü., Morkoc, H.: Transparent conducting oxides for electrode applications in light emitting and absorbing devices, Superlattice. Microst., 84, 458 – 84, (2010).

4 Hosono, H.: Recent progress in transparent oxide semiconductors: materials and device applications, Thin Solid Films, 515, 6000 – 14, (2007).

5 Gordon, R.G.: Criteria for choosing transparent conductors, MRS Bull., 25, [8], 52 – 7, (2000).

6 Straue, N., Rauscher, M., Roosen, A.: Preparation of nanosized ITO-dispersions and their printing via micro molding in capillaries, cfi/Ber. DKG, 86, [13], E33 – 39, (2009).

7 Gläser, H.J.: Large area glass coating; Von Ardenne Anlagentechnik Dresden, 2005.

8 Molpeceres, C., Lauzurica, S., Ocana, J.L., Gandia, J.J., Urbina, L., Cárabe, J.: Microprocessing of ITO and a-Si thin films using ns laser sources, J. Micromech. Microeng., 15, 1271 – 8, (2005).

9 Kuang, Z., Perrie, W., Liu, D., Fitzsimons, P., Edwardson, S.P., Fearon, E., Dearden, G., Watkins, K.G.: Ultrashort pulse laser patterning of indium tin oxide thin films on glass by uniform diffractive beam patterns, Appl. Surf. Sci., 258, 7601 – 6, (2012).

[10] Chung, Y.C., Chiu, Y.H., Liu, H.J., Chang, Y.F., Cheng, C.Y., Hong, F.C.N.: Ultraviolet curing imprint lithography on flexible indium tin oxide substrates, J. Vac. Sci. Technol. B, 24, [3], 1377 – 83, (2006).

[11] Kölpin, N., Wegener, M., Teuber, E., Polster, S., Frey, L., Roosen, A.: Conceptional design of nano-particulate ITO inks for inkjet printing of electron devices, J. Mater. Sci.; 48, 1623 – 31, (2013).

[12] Hwang, M.S., Jeong, B.Y., Moon, J., Chun, S.K.J., Kim, J.: Inkjet-printing of indium tin oxide (ITO) films for transparent conducting electrodes, J. Mater. Sci. Eng. B, 176, [14], 1128 – 31, (2011).

[13] Puetz, J., Aegerter M.A: Direct gravure printing of indium tin oxide nanoparticle patterns on polymer foils, Thin solid films, 516, 4495 – 4501, (2008).

[14] Han, S.Y., Herman, G.S., Chang, C.-H.: Low temperature, high-performance, solution-processed indium oxide thin-film transistors, J. Am. Chem. Soc., 133, 5166 – 9, (2011).

[15] Shimoda, T., Matsuki, Y., Furusawa, M., Aoki, T., Yudasaka, I., Tanaka, H., Iwasawa, H., Wand, D., Miyasaka, M., Takeuchi, Y.: Solution-processed silicon films and transistors, Nature, 440, [7085], 783 – 6, (2006).

[16] Hidber, P.C., Graule, T.J., Gauckler, L.J.: Citric acid- a dispersant for aqueous alumina suspensions, J. Am. Ceram. Soc., 79, [7], 1857 – 67, (1996).

[17] Roduner, E.: Size matters: why nanomaterials are different, Chem. Soc. Rev., 32, 583 – 92, (2006).

[18] Maksimenko, I., Gross, M., Königer, T., Münstedt, H., Wellmann, P.J.: Conductivity and adhesion enhancement in low-temperature processed indium tin oxide/polymer nanocomposites, Thin Solid Films, 518, [10], 2910 – 5, (2010).

[19] Nayak, P.K., Yang, J., Kim, J., Chung, S., Jeong, J., Lee, C., Hong, Y.: Spin-coated Ga-doped ZnO transparent conducting thin films for organic light-emitting diodes, J. Phys. D: Appl. Phys., 42, 035102, (2009).

[20] Straue, N., Rauscher, M., Dressler, M., Roosen, A.: Tape casting of ITO green tapes for flexible electroluminescent lamps, J. Am. Ceram. Soc., 95, [2], 684 – 9, (2012).

[21] Straue, N., Prado, S., Polster, S., Roosen, A.: Profile rod technique: continuous manufacture of submicrometer-thick ceramic green tapes and coatings demonstrated for nanoparticulate zinc oxide powders, J. Am. Ceram. Soc., 94, [6], 1698 – 1705, (2011).

[22] Krebs, F.C.: Review: fabrication and processing of polymer solar cells: a review of printing and coating techniques, Sol. Energ. Mat. Sol. C., 93, 394 – 412, (2009).

[23] Krebs, F.C., Tromholt, T., Jorgensen, M.: Upscaling of polymer solar cell fabrication using full roll-to-roll processing, Nanoscale, 2, 873 – 86, (2012).

[24] Sondergaard, R.R., Hösel, M., Jorgensen, M., Krebs, F.C.: Fast printing of thin, large area, ITO free electrochromics on flexible barrier foil, J. Polym. Sci. Pol. Phys., 51, 132 – 6, (2013).

[25] Wegener, M., Gillert, M., Durst, F., Roosen, A.: Fabrication of functional nanoparticulate coating in the submicrometre range with the slot die process, cfi/Ber. DKG, 90, [10], E35 – 42, (2013).

[26] Blankenburg, L., Schultheis, K., Schache, H., Sensfuss, S., Schrödner, M.: Reel-to-reel wet coating as an efficient up-scaling technique for the production of bulk-heterojunction polymer solar cells, Sol. Energ. Mat. Sol. C., 93, 476 – 83, (2009).

[27] Chu, W.-B., Yang, J.-W., Wang, Y.-C., Liu, T.-J., Tiu, C., Guo, J.: The effect of inorganic particles on slot die coating of poly(vinyl alcohol) solutions, J. Colloid Interf. Sci., 297, [1], 215 – 25, (2006).

[28] Wengeler, L, Schmidt-Hansberg, B., Peters, K., Scharfer, P., Schabel, W.: Investigations on knife and slot die coating and processing of polymer nanoparticle films for hybrid polymer solar cells, Chem. Eng. Process., 50, 478 – 82, (2011).

[29] Liu, M., Zhou, H.-Q. Zhu, H.-K., Yue, Z.-X., Zha, J.-X.: Tape casting of borosilicate glass/Al_2O_3 composites for LTCC substrate with various relative molecular masses of PVB. J. Cent. South Univ. T., 20, [1], 37 – -43, (2013).

[30] Wang, H., Qiao, X., Chen, J., Wang, X., Ding, S.: Mechanisms of PVP in the preparation of silver nanoparticles, Mater. Chem. Phys., 94, 449 – 453, (2005).

[31] Wegener, M., Lenhart, M., Roosen, A.: Processing nanoscale powders for the production of TCO coatings with high electrical conductivity and optical transparency, (in German), Chapter 3.3.3.10 in Technische Keramische Werkstoffe, Editors: Prof. Dr. Jochen Kriegsmann, HvB-Verlag (2015), 1 – 22.

[32] Wegener, M., Kato, M., Kakimoto, K., Roosen, A.: PVP as binder for the manufacture of ultrathin ITO/polymer nanocomposite films with improved electrical conductivity, J. Mater. Sci. 2015 DOI 10.1007/s10853 – 015 – 9168 – 9

[33] Carvalho, M.S., Kheshgi, H.S.: Low-flow limit in slot coating: theory and experiment, AIChE J., 46, [10], 1907 – 17, (2000).

[34] Young, T.: An essay on the cohesion of fluids, Phil. Trans. R. Soc. Lond., 95, 65 – 7, (1805).

[35] Mischke, P.: Film formation in modern paint systems, (in German), Vincentz Network, Hannover, Germany, (2007).

[36] Königer, T., Münstedt, H.: Influence of polyvinylpyrrolidone on properties of flexible electrically conducting indium tin oxide nanoparticle coatings, J. Mater. Sci. 44, 2736 – 42, (2009).

[37] Hotza, D., Greil, P.: Review: aqueous tape casting of ceramic powders, Mater. Sci. Eng. A – Struct., 202, 206 – 17, (1995).

[38] Roosen, A., Hessel, F., Fischer, H., Aldinger, F.: Interaction of polyvinylbutyral with alumina, Ceram. Trans., 12, 451 – 9, (1990).